Optimization of a Hybrid Energy System with District Heating and Cooling Considering Off-Design Characteristics of Components, an Effort on Optimal Compressed Air Energy Storage Integration

Chen, Shang; Arabkoohsar, Ahmad; Chen, Guodong; Nielsen, Mads Pagh

Published in:
Energies

DOI (link to publication from Publisher):
10.3390/en15134634

Publication date:
2022

Document Version
Publisher's PDF, also known as Version of record

energies

MDPI

Article

Optimization of a Hybrid Energy System with District Heating and Cooling Considering Off-Design Characteristics of Components, an Effort on Optimal Compressed Air Energy Storage Integration

Shang Chen [1,*], Ahmad Arabkoohsar [2,*], Guodong Chen [1] and Mads Pagh Nielsen [2]

[1] Technology Center, Shanghai Electric Power Transmission & Distribution Group Co., Ltd., Shanghai 200060, China; chengd@shanghai-electric.com
[2] Department of Energy Technology, Aalborg University, 9220 Aalborg, Denmark; mpn@et.aau.dk
* Correspondence: chenshang926@163.com (S.C.); ahm@energy.aau.dk (A.A.)

Abstract: In this work, the optimal design of a hybrid energy complex, including wind turbines, an internal combustion engine, and an adiabatic compressed air energy storage system is investigated. A novel bi-level optimization strategy is proposed for optimizing the capacity and operational power of each component of the system based on techno-economic considerations. The article presents information and discussions about the impacts of the partial-load operation of the energy storage system components on the optimal rated power and working strategies. The off-design characteristics are proven to have a huge negative impact on the efficiency and economy of the hybrid system. The efficiency reduction of the compressed air energy storage system is about 21% in summer and 8.9% in winter, when the system is operating in partial-load conditions. The operation cost of the system is reduced significantly when carrying out the proposed bi-level optimization strategy.

Keywords: compressed air energy storage systems; district heating and cooling; differential evolution; off-design performance

Citation: Chen, S.; Arabkoohsar, A.; Chen, G.; Nielsen, M.P. Optimization of a Hybrid Energy System with District Heating and Cooling Considering Off-Design Characteristics of Components, an Effort on Optimal Compressed Air Energy Storage Integration. *Energies* **2022**, *15*, 4634. https://doi.org/10.3390/en15134634

Academic Editor: Alan Brent

Received: 22 May 2022
Accepted: 21 June 2022
Published: 24 June 2022

1. Introduction

Energy storage systems are widely used for energy-load leveling today, but they will be much more broadly implemented and used in the future when renewable driven systems dominate [1]. Compressed air energy storage (CAES) has been shown to be one of those promising electricity storage technologies due to its low cost, long lifetime, and the established operation experience [2,3]. CAES was originally developed in the early 1960s, along with other gas expander technologies for power plants [4]. The first pilot CAES plant was a 290 MW unit located in Germany; it is a diabatic CAES that has been successfully operating for more than 40 years [5]. For diabatic CAES plants, the efficiency is in the range of 42% to 54%, mainly depending on the degree of recovery of the thermal energy in the system [6]. To improve the overall round-trip efficiency, adiabatic CAES (A-CAES) technology is proposed. In A-CAES, the thermal energy of the compression process is collected and stored to preheat the airflow before the expanders in the discharging hours, and the efficiency can be boosted up to 70% in this way [4].

For the best utilization of the CAES potential in energy stabilization, a variety of hybrid energy systems (HESs) integrated with this system are proposed. HESs that include renewable plants, an energy storage unit, and an auxiliary energy supply unit will be quite common in the future when the energy systems have to embrace more fluctuating renewable sources such as wind and solar. An example of such an HES is the wind farm connected to an A-CAES system and a flywheel energy storage system in [7]. There, the A-CAES system operates at variable cavern pressures and a constant turbine inlet pressure mode. The flywheel unit is controlled by a constant power strategy. In another effort,

a wind–diesel hybrid system with CAES is explored to reduce the diesel consumption of the generators with various penetration rates and give a higher power output of the diesel engine, resulting in a longer engine lifetime [8]. An energy system is proposed and investigated with real data to show the performance of a PV plant combined with CAES [9]. The energy and exergy efficiencies of CAES in an HES in this system are very close and vary from 35% up to 65% during the year. Furthermore, the HES as a city gate station has been studied in [10].

Various HESs are also proposed to show the potential of CAES for economy or efficiency improvement. The techno-economic analysis of CAES was presented to provide emergency back-up power to support a microgrid operation [11]. An economic benefit estimation model was developed to analyze the economic gains of CAES operation with different microgrid configurations, power supply reliabilities, and diesel prices. Exergoeconomic analysis was studied for a cogeneration system, including CAES, and the effects of the critical parameters, such as electricity purchase price, diurnal operating period, and the failure and repair rates on the cost of the products, were analyzed. The economic analysis revealed that the proposed system had a payback time of 2.9 years [12]. A cogeneration system composed of a CAES system, an organic Rankine cycle (ORC) cycle and an ejector system was proposed and investigated, leading to a round-trip efficiency of 72% in [13]. The integration of a CAES system with a gas turbine, an ORC, and an absorption chiller was built for energy and exergy analyses by Mohammadi et al. [14], showing a round-trip efficiency of about 54%. The techno-economic analysis of CAES was presented to provide emergency back-up power to support a microgrid operation. An economic benefit estimation model was developed to analyze the economic gains of CAES operation with different microgrid configurations, power supply reliabilities, and diesel prices. District energy systems can also be integrated with CAES systems to perform a 'peak shaving' function and maintain a stable power output. Such a hybrid system was proposed and studied in [15], with an exergy efficiency of 41.5% and a primary fuel saving ratio of 23%.

The optimization of the design and operation of such HESs is crucial to obtaining the expected outcomes. The cost and performances of HESs are the two main objectives for the optimization. Yan et al. [16] presented a multi-objective optimization algorithm for finding the optimal cost, energy efficiency, and environmental effect of an HES consisting of a trigeneration CAES unit. The HES was compared with a traditional combined cooling, heating, and power system (CCHP). An evolutionary multi-objective algorithm was developed in [17] to handle the trade-off between the cost and the exergy efficiency of another HES composed of a trigenerative CAES through Pareto solutions. A CAES system combined with an ORC unit and an ejector system was optimized, resulting in a round-trip efficiency growth of 5.7% compared to the base case [18]. In addition, a data-driven method was proposed to study one full year's worth of real operating data, and a new approach was introduced to design CAES based on specific grid requirements [19].

Naturally, the off-design operation of the components of an HES could have a significant effect on the optimal operation point and the size of the system components. This is of even more importance for the energy storage unit of an HES as it will frequently and inevitably go to partial-load conditions. A comprehensive analysis of the CAES system with low-temperature thermal storage under off-design conditions was presented by Guo et al. [20]. A case study, including wind turbine integrated with a CAES system, was investigated in [21]. The results showed that the partial-load fluctuations of the HES can be reduced. Mazloum et al. developed the dynamic modeling of an isobaric A-CAES (IA-CAES) based on the mechanical inertia of the compressors and the air turbines [22]. It was proved that the levelized cost of electricity of an A-CAES working in an off-design condition was significantly higher than that of an A-CAES operating at nominal load [23]. The round-trip efficiency of an A-CAES approaches 68% at a nominal load, while it offers the lower efficiencies of 52% and 28% if working at 50% and 10% loads, respectively [24]. In the case of the subcooled-CAES, the overall coefficient of performance of the system will

decrease to 1.27 and 1.05 if the operational load drops to 50% and 10%, respectively, while it can reach a value of above 1.6 at nominal-load operation [25].

The fact is that the literature so far has considered the optimization of HESs in rated conditions. Off-design analyses are seldom applied to obtain the optimal capacity of each device and operation strategy of HESs. With the fluctuating data and multi-energy streams in the system, the devices operate with different power outputs. Thus, a novel HES that includes wind turbines, an A-CAES, and an internal combustion engine (ICE) for district heating, cooling, and power is investigated in this paper. For CAES especially, coupling with WTs, ICE, and other devices should operate in an off-design condition. The capacity of the system components and operational strategy of the ICE and A-CAES is optimized as the optimal efficiency and economy of the system is the objective. A novel bi-level optimization strategy is introduced and applied for the optimization. In particular, the off-design characteristics of A-CAES and ICE are considered so that the optimal results could approach the actual operation condition. Finally, the performance of the A-CAES unit and the economy of the HES are investigated.

2. Methodology

The proposed system for supplying the CCHP energy is shown in Figure 1. In the HES, the wind turbines (WT) are the main source of the electricity load, and the ICE with heat recovery and an absorption chiller produces the electricity, heating, and cooling load. Due to the fluctuation of the WT power generation and the user load, there is extra or a lack of power, and the A-CAES is employed in the system to balance the energy. There are two processes of the A-CAES: the charging and the discharging processes.

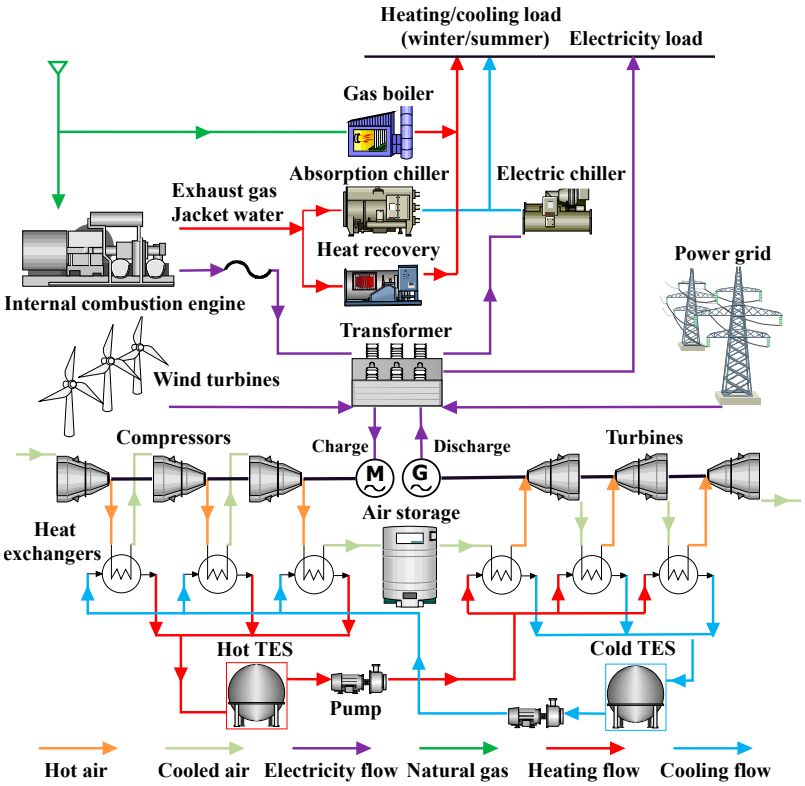

Figure 1. The structure of the HES with CAES.

In the charging process, when the generation power is higher than the electricity load, the surplus power can be stored with the compressors by producing compressed air. The heat of the compressed air is recovered by heat exchangers with the water from the cold Thermal Energy Storage (TES), and the heated water is charged into hot TES. The heat exchanger is arranged after each compressor. Through 3-stage compression, the

compressed air can be charged into the air storage chamber. In the discharging process, the generation power is less than the electricity load, and the high-pressure air is discharged from an air storage chamber and heated up in a heat exchanger by the water from the hot TES. The heat exchanger is arranged before each turbine. Then, the air expands in the turbine, through 3-stage expansion, to generate electricity. The enthalpy of the air drops a lot after the expansion so that the temperature of the expanded air is low enough to supply the cooling load. If the generation power of the WT and A-CAES is still not able to meet the electricity load, the lack of the power can be supplied by an ICE. The heat of the exhaust gas and the jacket water of the ICE are recovered, and the heat recovered from the ICE is also used to supply the cooling load through an absorption chiller. In addition, the power grid, gas boiler, and electric chiller are used to compensate for the lack of the electricity, heating, and cooling load.

The novel bi-level strategy of the optimization model of the total daily cost is introduced in this section and is shown in Figure 2.

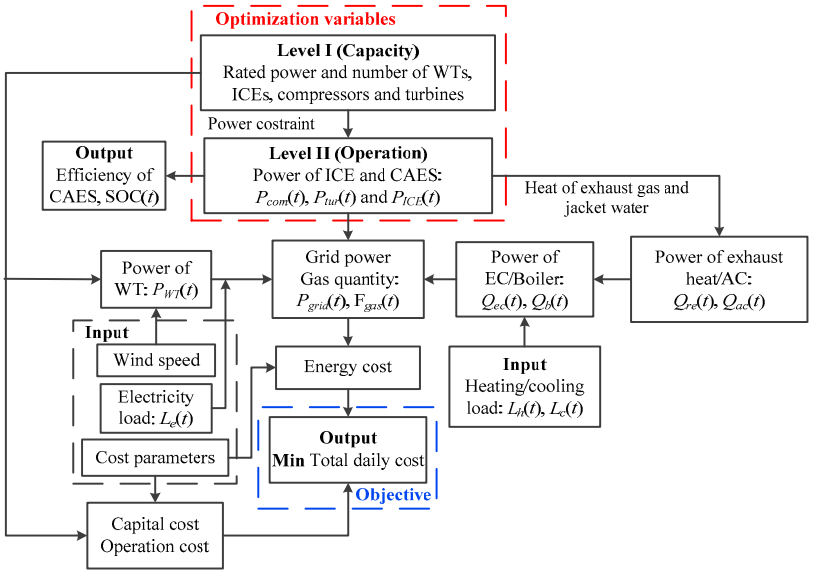

Figure 2. Calculation strategy of the HES with CAES.

The bi-level optimization strategy can be divided into two levels: at Level I, the rated power and the number of WTs, ICEs, compressors, and turbines of the A-CAES should be optimized; at Level II, the power of the ICEs, compressors, and turbines of the A-CAES should be optimized. The optimization result of Level I is the constraint condition of Level II. Through the Level I results, with the inputting of the data of the wind speed at each hour, the operational power of the WT can be calculated. Through the Level II results, the gas quantity and the power of the recovery heat/absorption chiller (AC) of the ICE can be calculated, and with the inputting of the data of the heating/cooling load, the power of the boiler and electric chiller (EC) can be obtained. Then, with the inputting of the data of the electricity load, the grid power can be calculated. Finally, with the inputting of the data of the cost parameters, the capital cost and the operational cost of the system can be calculated. The optimization objective of Level I is the minimum capital cost.

At Level II, the power, cooling, and heating quantity at each hour can be calculated with the energy balance equations. For Level II, the minimum energy cost is the optimization objective. The power of each energy supply device can be calculated using thermodynamic models. The recovered heat can be calculated by $P_{ICE}(t)$; so, the lack of heat or cooling load should be supplied by the boiler or chiller. Then, the gas cost can be obtained with the gas price data. In addition, the input power of the compressors and the output power of the WTs, turbines, and ICE can be carried out to calculate the electricity

that should be purchased from the grid; so, the electricity cost can be obtained with the energy price data.

Finally, the total daily cost can be calculated for optimization. In order to carry out the above calculation, the mathematical model is presented in the next section. Some assumptions are made to simplify the analysis of the model.

a. Air can be regarded as an ideal gas; it meets the ideal gas state equation.
b. The properties of the fluids are considered to be constant.
c. The heat loss and pressure drop in the pipes are ignored.
d. The throttling process is isenthalpic.

3. Mathematical Models

Thermodynamics is employed to build the mathematical models of each device in the system, and the operational power of each generator at time t is given in this section.

a. WT Model

The mathematical model of the WT is shown by the following functions [17]:

$$P_{WT}(t) = \begin{cases} 0, & v(t) \le v_{in} \quad or \quad v(t) \ge v_{out} \\ \frac{v^3(t)-v_{in}^3}{v_r^3-v_{in}^3} P_r, & v_{in} \le v(t) \le v_r \\ P_r, & v_r \le v(t) \le v_{out} \end{cases} \tag{1}$$

where $P_{WT}(t)$ and $v(t)$ are the operational power of the WT and wind velocity. P_r is the rated power; v_r is the rated wind speed; v_{in} is the cut-in speed; and v_{out} is the cut-off speed.

b. ICE Model

The gas consumption model of the ICE can be estimated as [16]:

$$G_{ICE}(t) = \frac{P_{ICE}(t)}{\eta_{pe}(t)\eta_{te}(t)} \tag{2}$$

where $G_{ICE}(t)$ represents the gas consumption rate when the generating power is $P_{ICE}(t)$ at the time t; $\eta_{pe}(t)$ and $\eta_{te}(t)$ are the electricity and thermal efficiency. The waste heat can be expressed as

$$G_{ICE}(t)(1-\eta_{te}(t)) = Q_{jw}(t) + Q_{ex}(t) + Q_{loss}(t) \tag{3}$$

where $Q_{jw}(t)$ is the jacket water heat, $Q_{exh}(t)$ is the exhaust heat, and $Q_{loss}(t)$ is the heat loss which is caused by the oil cooler and thermal radiation. Thus, we define $Q_{re}(t)$ as the waste heat recovery of the system, and the waste heat balance can be represented as

$$Q_{re}(t) = Q_{jw}(t)\eta_{jw}(t) + Q_{exh}\eta_{exh}(t) \tag{4}$$

where η_{jw} and η_{exh} represent the efficiency of the jacket water heat exchanger and the exhaust heat exchanger, respectively. Table 1 presents the partial-load ratio (PLR) performance of the ICE (GE J320GS, 1067 kW). f_{jw}, f_{ex}, f_{ic}, and f_{loss} denote the coefficients corresponding to jacket water heat, exhaust gas heat, intercooling, and heat loss.

c. CAES Model

For the off-design performance of turbomachines, four important characteristics variables exist that could affect each other. These are the flow rate through the turbomachine, its isentropic efficiency, the pressure ratio, and the speed of rotation. Here, the rotational speed is considered to be constant at any operating load, and thus, the parameters being affected by the off-design operation are reduced to three (i.e., pressure ratio, isentropic efficiency, and flow rate). The variation of the flow rate is represented here by the load of the operation (% of the nominal flow rate). In Figures 3 and 4, the plots made by the curve fitting on the performance maps of real-life compressors and turbines [26,27] show

the variation of these three parameters in relation to each other for the compressor and the turbine used in this study.

Table 1. Performance factors of ICE.

PLR	η_{pe}	η_{te}	f_{jw}	f_{ex}	f_{ic}	f_{loss}
50%	0.3824	0.9653	0.3236	0.5245	0.1086	0.0432
60%	0.3915	0.9744	0.3210	0.5154	0.1235	0.0401
75%	0.4019	0.9720	0.2953	0.5191	0.1489	0.0366
85%	0.4067	0.9742	0.2702	0.5039	0.1871	0.0388
100%	0.4113	0.9744	0.2536	0.5125	0.1966	0.0373

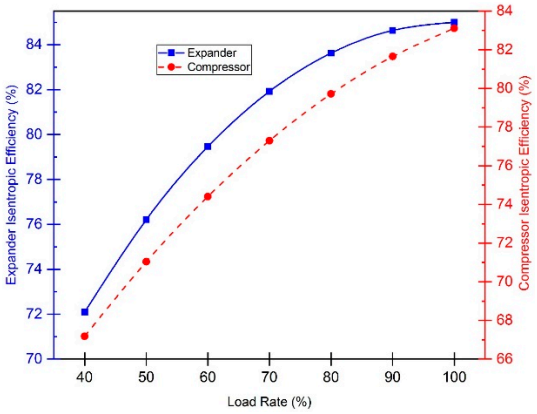

Figure 3. Isentropic efficiency of the compressors and turbines versus the load of operation.

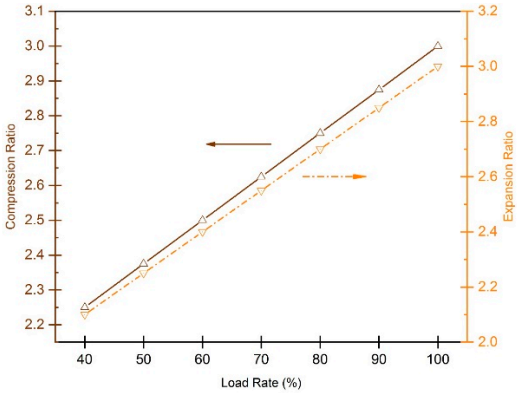

Figure 4. Compression/expansion ratio of compressors/expanders at various load levels.

At time t, the model is built to calculate the performance of the A-CAES. The partial-load ratio $\alpha_{c,pl}$ (t) is proposed to investigate the off-design performance of the compressor:

$$\alpha_{c,pl}(t) = \frac{P_c(t)}{P_{c,r}} \tag{5}$$

where $P_c(t)$ and $P_{c,r}$ are the operational and rated power of the compressor. Through the performance curve in Figures 3 and 4, the efficiency of the compressor $\eta_c(t)$ can be calculated. The pressure ratio of the compressor is set as π_c. If the air temperature of the compressor inlet is $T_{c,in}(t)$, then the definition of the air temperature of the compressor outlet $T_{c,out}(t)$ can be calculated with π_c and $\eta_c(t)$ as:

$$T_{c,out}(t) = T_{c,in}(t)\left(1 + \frac{1}{\eta_c(t)}\left(\pi_c^{\frac{\gamma-1}{\gamma}} - 1\right)\right) \tag{6}$$

where γ is the polytropic index as 1.4. As c_{pa} is the average specific thermal capacity of air, the specific work of the compressor $w_c(t)$ is defined as:

$$w_c(t) = c_{pa}(T_{c,out}(t) - T_{c,in}(t)) \tag{7}$$

The air mass flow rate $m_{c,a}(t)$ through the compressor of the A-CAES can be calculated using the following formula:

$$m_{c,a}(t) = \frac{P_c(t)}{w_c(t)} \tag{8}$$

The compressor is driven by the electricity from the system, and the electricity is defined as:

$$E_c = \int_0^{t_c} P_c(t) \cdot dt \tag{9}$$

where t_c is charging time, as:

$$t_c = \frac{V(p_{\max} - p_{\min})}{m_{c,a}(t) R_g T_0} \tag{10}$$

where V, p_{max}, and p_{min} are the volume and the maximum and minimum pressure of the storage chamber; T_0 is the air temperature in the air storage chamber at t_c = 0; and R_g is the air gas constant = 287 J/(kg·K).

The heat exchanger is employed to cool the compressed air after each compressor and heat the air before each turbine with cold and hot water, respectively, as shown in Ref. [28]; the ε is heat exchanger efficiency, defined as follows:

$$\varepsilon = \frac{c_{pa} m_a (T_{in,a} - T_{out,a})}{(c_p m)_{\min}(T_{in,a} - T_{in,w})} = \frac{c_{pw} m_w (T_{in,w} - T_{out,w})}{(c_p m)_{\min}(T_{in,a} - T_{in,w})} \tag{11}$$

where c_{pw} is the average specific thermal capacity of water, and m_a and m_w are the mass flow rate of the air and water in the heat exchanger, respectively. $T_{in,w}$ and $T_{out,w}$ are the inlet and outlet water temperature. $T_{in,a}$ is the inlet temperature of the air in. Assuming the hot air has the minimum heat capacity, the outlet air temperature $T_{a,he,out}$ is defined as follows:

$$T_{a,he,out} = (1 - \varepsilon) T_{a,he,in} + \varepsilon T_{w,he,in} \tag{12}$$

where $T_{w,he,in}$ is the inlet water temperature.

In the heat exchanger, the pressure loss can be calculated as the empirical equation [29]:

$$\Delta p = \left(\frac{0.0083\varepsilon}{1 - \varepsilon} \right) p_{in} \tag{13}$$

where Δp is pressure loss in the heat exchanger, and p_{in} is the inlet air pressure of the heat exchanger.

As a gas–fluid heat exchanger, the ε is quite high and can be 0.95 at the nominal load. Additionally, in order to maintain the outlet temperature of the heat exchanger constantly at any other operational load, there should be pumps before the outlet of the heat exchangers to adjust the flow rate of the water. When the load is lower than the nominal load, the work of the pump will be lower. Here, the pump work is much smaller compared to that of the compressors and the turbines; so, a linear work drop in accordance with the level of load decrease is favorable. The rate of electricity consumption of the pump can be calculated by [25]:

$$W_{pump} = \frac{m_w \Delta p_{pump}}{36 \rho_w \eta_{pump}} \tag{14}$$

where ρ_w, Δp_{pump}, and η_{pump} are the water density, the pressure difference of the two sides of the pump, and the overall pump efficiency.

The partial-load ratio $\alpha_{t,pl}(t)$ is proposed to investigate the off-design performance of the turbine; when the operational and rated power of the turbine are $P_t(t)$ and $P_{t,r}$, $\alpha_{t,pl}(t)$ can be calculated as:

$$\alpha_{t,pl}(t) = \frac{P_t(t)}{P_{t,r}} \tag{15}$$

Through the performance curve in Figures 3 and 4, the efficiency of the turbine $\eta_t(t)$ can be calculated. The expansion ratio of the turbine is set as π_t. To define the air temperature of the turbine outlet $T_{t,out}(t)$, it can be calculated with π_t and $\eta_t(t)$ as:

$$T_{t,out}(t) = T_{t,in}(t)\left(1 - \eta_{t,i}(t)\left(1 - \pi_t^{\frac{1-\gamma}{\gamma}}\right)\right) \tag{16}$$

where $T_{t,in}(t)$ and $w_c(t)$ are the inlet air temperature and the specific work of the turbine, and $w_c(t)$ is defined as:

$$w_t(t) = c_{pa}(T_{t,in}(t) - T_{t,out}(t)) \tag{17}$$

The air mass flow in the turbine $m_{t,a}$ is defined as:

$$m_{t,a}(t) = \frac{P_t(t)}{w_t(t)} \tag{18}$$

Similar to the compressor in the charging process, the electricity generated from the turbine is defined as:

$$E_t = \int_0^{t_t} P_t(t) \cdot dt \tag{19}$$

where t_t is the discharging time, defined as:

$$t_t = \frac{V(p_{\max} - p_{\min})}{m_{t,a}(t) R_g T_0} \tag{20}$$

In terms of efficiency, the overall CAES system efficiency η_{CAES} can be defined as follows:

$$\eta_{CAES} = \frac{E_t}{E_c} \tag{21}$$

The state of charge (SOC) can present the feasibility and safety of the dispatch plan for the A-CAES, and it can be defined as [16]:

$$\mathrm{SOC} = \frac{m_{ch}(t) - m_{\min}}{m_{\max} - m_{\min}} \tag{22}$$

$$m_{\min/\max} = \frac{p_{\min/\max} V}{R_g T_0} \tag{23}$$

$$m_{ch}(t) = m_{\min} + \sum_{i=0}^{t} m_{c,a}(i) - \sum_{i=0}^{t} m_{t,a}(i) \tag{24}$$

In order to be integrated in the HES, the motor of the compressors and the generator of the turbines are used in the A-CAES. As the optimization variable in the calculation, the operational power $P_{CAES}(t)$ of the A-CAES is calculated by Equation (25),

$$P_{CAES}(t) = \begin{cases} P_c(t)/\eta_m & Charging \\ -P_t(t)\eta_g & Discharging \end{cases} \tag{25}$$

where the $\eta_m(t)$ and $\eta_g(t)$ are the efficiency of the motor and the generator, set as 0.95, respectively. In the charging process, the $P_{CAES}(t)$ is set as a positive value, and in the discharging process, the $P_{CAES}(t)$ is set as a negative value.

d. Constraints

For the mathematic model, there are constraints for the CAES and the ICE:
(a) Storage constraints of the CAES:

$$p_{\min} \leq p_{ch} \leq p_{\max} \tag{26}$$

$$0 \leq \mathrm{SOC} \leq 1 \tag{27}$$

(b) Power constraints of the compressors, turbines, and the ICEs:

$$\begin{cases} 0 \leq P_{com} \leq P_{com,r} \\ 0 \leq P_{tur} \leq P_{tur,r} \\ 0 \leq P_{ICE} \leq P_{ICE,r} \end{cases} \tag{28}$$

where $P_{com,r}$, $P_{tur,r}$, and $P_{ICE,r}$ are the rated power of the compressors, turbines, and ICEs, respectively.

e. Energy balance model

The heating and cooling power load is supplied from the WT, A-CAES, and ICE, and the power energy balance is defined as:

$$P_{WT}(t) + P_{CAES}(t) + P_{ICE}(t) + P_{grid}(t) = L_e(t)(+P_{ec}(t)) \tag{29}$$

where $P_{WT}(t)$, $P_{CAES}(t)$, and $P_{ICE}(t)$ are the powers of the WT, A-CAES, and ICE, respectively; $P_{grid}(t)$, $L_e(t)$, and $P_{ec}(t)$ and $P_{com}(t)$ are the powers of the grid, the user load, and the electric chiller.

The heat energy load $L_h(t)$ is supplied by the recovery heat of the ICE $Q_{re}(t)$ and the heat of the gas boiler $Q_b(t)$; the heat balance is defined as:

$$Q_{re}(t) + Q_b(t) = L_h(t) \tag{30}$$

The cooling energy load $L_c(t)$ is supplied by the power of the AC $Q_{ac}(t)$ and the EC $Q_{ec}(t)$ and is defined as:

$$Q_{ac}(t) + Q_{ec}(t) = L_c(t)/COP \tag{31}$$

where COP is the coefficient of the AC.

f. Economic model

The aim of the model is to obtain the minimum total daily cost C_{td}, which is defined as:

$$C_{td} = C_{ca} + C_{en} + C_{op} \tag{32}$$

where C_{en} and C_{op} are the energy cost and the operation cost, respectively. C_{ca} is the capital cost, which is defined as

$$C_{ca} = C_{ac} P_f \frac{d(1+d)^L}{(1+d)^L - 1} \tag{33}$$

where C_{ac}, L, and P_f are the acquisition cost factor, the lifespan, and the rated power of the device, and d is the discount rate with the range of value (0.1).

The energy cost consists of the costs of the natural gas $C_{gas,i}$ and the electricity $C_{ele,i}$ and is defined as

$$C_{en} = \sum_{i=1}^{t} \left(C_{gas,i} + C_{ele,i} \right) \tag{34}$$

The operation cost consists of the operation and maintenance (O&M) costs:

$$C_{op} = C_{OM,WT} + C_{OM,ICE} + C_{OM,CAES} \tag{35}$$

The default values of the parameters for the cost calculation are given in Tables 2 and 3 [16]. For the lifespan assumption, the replacement of the spare parts is ignored. The acquisition is considered as a one-time investment. The O&M is considered to be the same in each year. With the proposed models above, in terms of the validation and real simulation values, the models of the system are all acceptable and realistic.

Table 2. Parameters of the capital cost.

Parameters	WT	ICE	CAES
Acquisition cost (USD/kW)	770	812	325
O&M cost (USD/h)	1.2	0.3	0.16
Lifespan (year)	20	10	10

Table 3. Parameters of the energy prices.

Parameters	Time	Price
Electricity (USD/(kW h))	11:00–14:00, 18:00–23:00	0.168
	7:00–11:00, 14:00–18:00	0.108
	23:00–7:00	0.057
Natural gas (USD/(kW h))	All day	0.035

4. Results and Discussion

In China, the research on storage technology has become more and more important as renewable energy is currently developing rapidly. CAES is one of the most acceptable systems and has had many trials for engineering applications. For example, a 6 MW system has been built by the Institute of Engineering Thermophysics; it is enough for engineering applications [30], and a 100 MW system is now ready to be built for realistic applications. Additionally, considering the energy supply of power, heating, and cooling for on-site needs, CAES with a high level of dynamic performance also has engineering applications in China [15]. Thus, in this paper, the proposed HES with CAES is feasible for the engineering applications. A real case, with the energy data of Chongming county in Shanghai, China, is presented to design the HES with the power, heating, and cooling load with the method proposed in this article [31]. Figures 5 and 6 show the inputting of the data of the wind speed, electricity, and cooling loads of a typical summer and winter day, respectively. In both seasons, the rated power and operational power of each device should be optimized simultaneously. The comparison of the model with and without the off-design characteristics can be carried out through the optimal results in different seasons and is implemented with the program in Fortran.

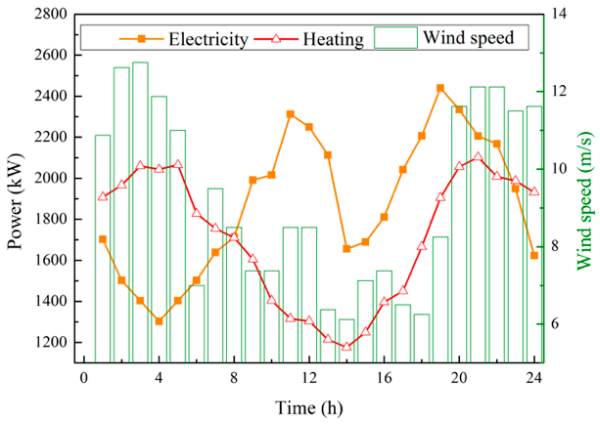

Figure 5. Inputting data in summer.

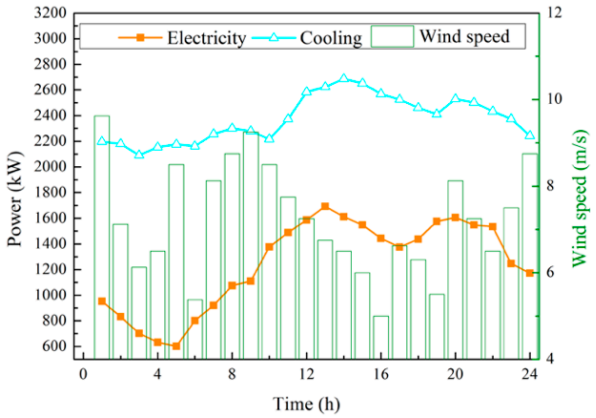

Figure 6. Inputting data in winter.

In this paper, the differential evolution (DE) algorithm is used as the optimization method to find the optimal objectives. DE was chosen because this method promises simple, fast, and robust optimization [32]. The authors have conducted the optimization and synthesis studies on A-CAES based on DE algorithms [33]. In this optimization, DE is employed with particular specifications (population size 500, mutation factor 0.5, and crossover factor 0.1 for optimizing the five key decision variables: the capacities of the compressors, turbines, and WTs and the operation loads of the compressors and turbines).

The daily cost of the system in different seasons is the objective of the optimization in level II, and the one-day efficiency of the CAES is another system performance that is observed with each iteration when the system is optimized. As shown in Figure 7, the operation cost of the system decreases with the growing number of iterations. The one-day efficiency of the CAES is also presented along with each iteration, which increases a lot at first, to about 35% for the off-design case and 51% for the case that does not consider the off-design operation, and then, it approaches a stable value. When considering the off-design characteristics with a fixed capacity of the components, the one-day efficiency of the CAES drops to 30.4%. When employing the bi-level optimization strategy, the efficiency increases to 35.7% in the off-design operation. The optimal cost is the sum of the daily costs of the typical winter and summer conditions. When the off-design characteristics are not considered, the optimal cost of the system is USD 6882, which is lower than the cost of the system when considering the off-design characteristics; when the capacity is fixed and when employing the bi-level optimization, the costs are USD 7007 and USD 6989, respectively.

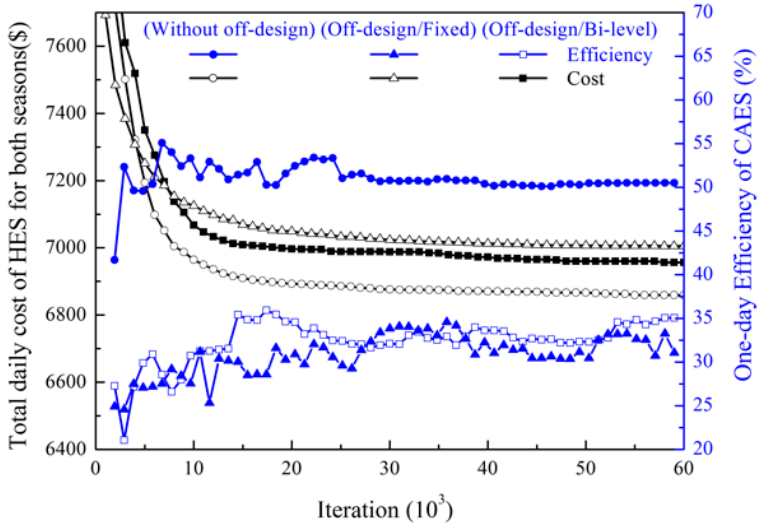

Figure 7. The optimization characteristics curves of different parameters in level II.

The default values of the thermodynamic parameters and the optimization results (rated power and number) of the WT, ICE, and A-CAES are shown in Table 4. In Figure 8, for level I, the optimization curve of the rated power is presented. For the off-design case, the rated power of the WTs is 1523 kW, which is higher than that for the case that does not consider the off-design characteristics, whose power is 1493 kW. Conversely, the turbines are 130 kW in the off-design case, which is lower than the turbines that do not consider the off-design characteristic, whose power is 144 kW. When it comes to a partial-load value, the operation power of the compressors should be higher to obtain higher efficiency, leading to the higher power of the WTs; so, the optimal rated power of the WTs increases. The value of the devices varies with the iteration in level I, and the fluctuation of the rated power of the WT is higher than that of the turbines and compressors.

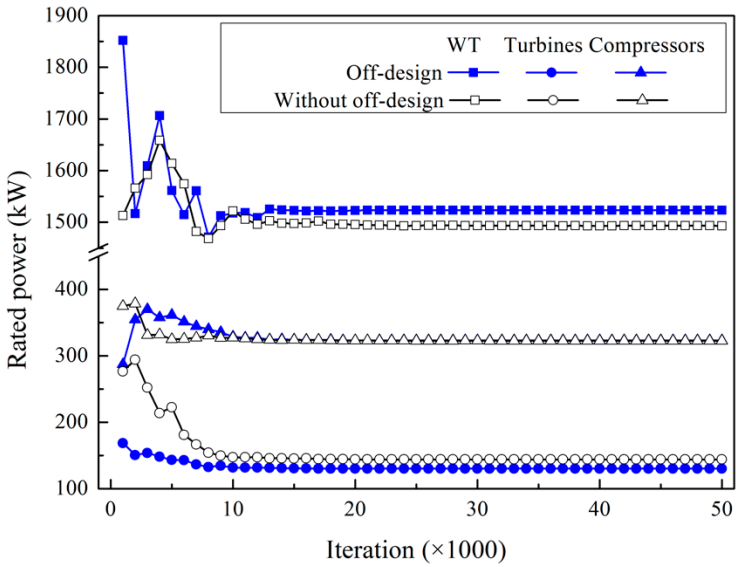

Figure 8. The optimization characteristics of the rated power in level I.

In addition, the operation time of the compressors will be less if they should maintain high efficiency in one day. Thus, less extra energy will be charged into the chamber, leading to lower turbine power for discharging. From the results, the main effect of the bi-level strategy is to optimize the rated power and the operational power of the devices simultaneously. Although the off-design characteristics could affect the performances of the CAES, a better configuration could avoid the operation of the devices too far away from the rated condition.

The optimal results obtained for the different cases are shown in Table 5. The total daily costs of the case that does not consider the off-design characteristics are USD 3032 in summer and USD 3850 in winter), which are lower than those of the case that considers the off-design characteristics (USD 3076 in summer and USD 3913 in winter), when the capacity is fixed. The deviation between the operation cost of the two cases is 4.8% in summer and 2.7% in winter. Obviously, the off-design characteristics have an effect on the system when obtaining an economic operation. Moreover, when employing the bi-level optimization strategy, the operation cost decreases to USD 1360, and the capital cost increases to USD 1716, when compared to the fixed capacity. Then, the total daily cost of the case optimized by the bi-level strategy is lower than the case with the fixed capacity when considering the off-design condition. So, the strategy can reduce the impact of the off-design characteristics by increasing the capacity of the devices, and the deviation of the operation cost between the cases with and without the consideration of the off-design characteristics can decrease from 4.8% to 1.3%. The decrease between the deviation of the operation cost under the bi-level strategy and the fixed capacity could be 73%. Thus, if considering the off-design features, when the devices operate too far away from their rated power (capacity) their

efficiency drops considerably and leads to more cost. The bi-level strategy succeeds in optimizing the capacity and the operation of the devices simultaneously.

Table 4. Performance parameters of devices.

Device	Parameters	Values
WT	v_{in} (m/s)	3
	v_r (m/s)	12
	v_{out} (m/s)	25
	Rated power with/without off-design (kW)	1523/1493
	Number	3
ICE	P_{rated} (kW)	1067
	$T_{exhaust}$ (°C)	460
	$m_{exhaust}$ (kg/h)	5688
	Forward/return $T_{jacket\ water}$ (°C)	93/75
	$m_{jacket\ water}$ (m^3/h)	31
	Number	1
Compressor	Rated power with/without off-design (kW)	323/323
	Pressure ratio	3.7
	Stage number	3
Turbine	Rated power with/without off-design (kW)	130/144
	Pressure ratio	3.3
	Stage number	3
Air storage chamber	Volume (m^3)	2000
	$p_{\max}/p_{\min}$ of storage chamber (bar)	50/35
Cooling/Heating	ε	0.7
	COP_{AC}	1.4
	COP_{EC}	5
	$\eta_{gas\ boiler}$	0.91

In summer, the one-day efficiency of the CAES, $\eta_{1\text{-day}}$, when considering the off-design characteristics, decreases by 40.2% compared to that of the case that does not consider the off-design characteristics, while the deviation is 39.2% in winter when the capacity is fixed. It can be seen that the off-design characteristics have less of a side effect on the efficiency of the CAES in winter, for the reason that extra wind energy can be supplied to the compressor so that it can operate closer to nominal power and store more energy for turbine operating. In addition, after employing the bi-level optimization, the deviation of the $\eta_{1\text{-day}}$ between the cases with and without considering the off-design characteristics decreases to 42.6% in summer and 11.5% in winter. In order to investigate the off-design characteristics of the CAES more deeply, the following calculations are all carried out with the bi-level optimization algorithm.

The off-design characteristics also have an impact on the outlet of the compressors; lower partial load leads to lower isentropic efficiency. If the air temperature of the compressor outlet is higher, then the temperature of the thermal fluid will be higher. Thus, as shown in Figure 9, for the off-design case, the mean temperature in the thermal storage chamber (at least 490 K and 457 K in winter and summer, respectively) is higher than that for the case that does not consider the off-design characteristics (475 K and 443 K in winter and summer, respectively). In particular, the mean temperature in the time period from 07:00 to 19:00 is relatively higher than the mean temperature at other times in the winter conditions, and the mean temperature increases after the time of 05:00 in the summer conditions. The reason for that is that the partial load of the compressor is much lower than the rated power; so, the isentropic efficiency of the compressor drops a lot, leading to the higher outlet air temperature.

Table 5. Optimal results.

	Cost and Efficiency	Without Off-Design	Fixed Capacity		Bi-Level	
			Off-Design	Deviation	Off-Design	Deviation
	Capital cost (USD)	1699	1699	0.0%	1716	1.0%
Summer	Operation cost (USD)	1332	1399	4.8%	1360	1.3%
	Total daily cost (USD)	3032	3098	2.1%	3076	1.5%
	$\eta_{1\text{-day}}$ of CAES	57.6%	34.4%	40.2%	36.6%	36.5%
Winter	Operation cost (USD)	2151	2210	2.7%	2197	2.1%
	Total daily cost (USD)	3850	3909	1.5%	3913	1.6%
	$\eta_{1\text{-day}}$ of CAES	43.6%	26.5%	39.2%	34.7%	20.4%

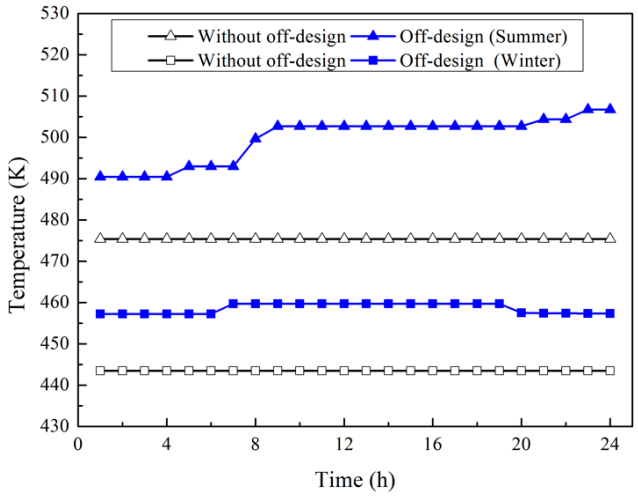

Figure 9. Mean temperature in the thermal storage chamber.

Figure 10 presents the SOCs of the cases with and without consideration of the off-design characteristics in summer or winter conditions. The maximum SOC of the chamber considering the off-design characteristics (43.6% in summer and 86.0% in winter) is 10.9% and 9.2% lower than that of the case that does not consider the off-design characteristics (54.5% in summer and 95.2% in winter), respectively. For one thing, more energy is charged and discharged by CAES in winter. This is mainly because the wind speed during winter is obviously higher than that in summer. Another thing worth noting is that the efficiency of the compressors and turbines will drop a lot if the power is lower than the rated power when they operate in a partial-load condition. In order to gain higher efficiency, the optimal operation load of the compressors and turbines will be closer to the rated power. The dispatching load of the other power generation utilities may not be enough to balance the energy, such as when there is not enough extra wind energy to supply the electricity for the compressors. Thus, the maximum storage ability of the CAES will drop when considering the off-design characteristics. However, when it comes to the case that does not consider the off-design characteristics, the range of the charging and discharging load can be wider. More energy can be stored, and the maximum SOC is higher when the case is ignoring the off-design characteristics.

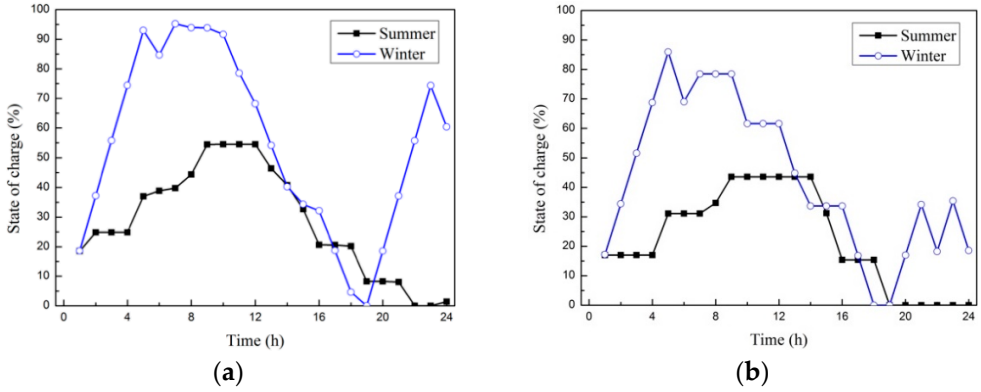

Figure 10. Comparison of SOCs between the cases with and without off-design effects consideration: (**a**) without considering off-design characteristics; (**b**) considering off-design characteristics.

The operational power of each device in summer is shown in Figures 11 and 12. In Figure 11, the negative values of the green columns come from the compressors in the charging process of the CAES, which mainly occurs at night. In contrast, the operational power of the turbines in the discharging process is shown by the yellow columns; this process mainly occurs when the load is higher (13:00–16:00, 19:00, 22:00). The CAES mainly absorbs the electricity generated by the WT in the charging process. The grid power is also stored, as can be seen in the dark green column in Figure 11a, at 02:00 and 06:00, when considering the variety of the electricity price. As shown in Table 4, the maximum powers of all the compressors for the cases without and with consideration of the off-design characteristics are both 929 kW, and the powers of the turbines without and with consideration of the off-design characteristics are 432 kW and 390 kW, respectively. There are 8 charging hours and 6 discharging hours in Figure 11a, while there are 4 charging times and 3 discharging times in Figure 11b. Obviously, less energy is charged and discharged in the case considering the off-design characteristics. However, the partial-load ratio of the compressors and the turbines is higher in Figure 11b than that without the consideration of the off-design characteristics. The minimum partial-load ratios of the compressor and the turbine of the CAES considering the off-design characteristics are 27.9% and 61.3%, respectively, while those of the case without consideration are 4.9% and 39.6%. Thus, when the optimization considers the off-design characteristics, the operation power of the device is closer to its nominal power.

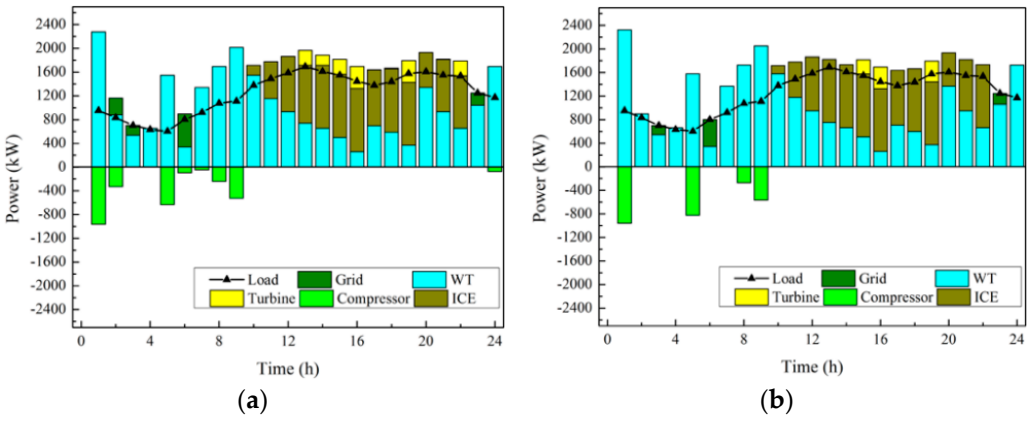

Figure 11. Operational power of electricity in summer: (**a**) without considering off-design characteristics; (**b**) considering the off-design characteristics.

Figure 12 presents the operational power of the EC and the ICE-AC on a summer day. The cooling load is mainly supplied by the electric chiller. In the time period (10:00–22:00), half of cooling load can be supplied by the absorption chiller with the recovered heat from the ICE. The off-design characteristics of the A-CAES have no effect on this part.

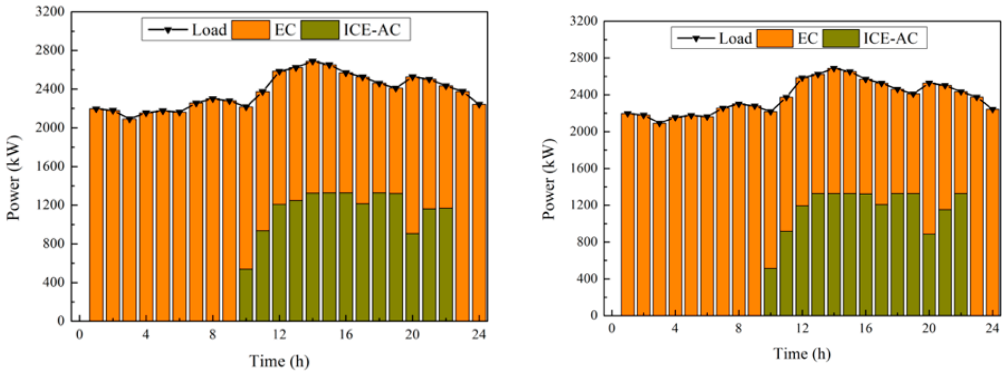

Figure 12. Operational power of heat in summer: (**a**) without considering off-design characteristics; (**b**) considering off-design characteristics.

In winter conditions, the optimal operational powers of each device in the system are presented in Figures 13 and 14. In Figure 13, there is no other electricity cost except the electricity of the user demand. There are 10 charging times and 10 discharging times in Figure 13a, while there are 9 charging times and 8 discharging times in Figure 13b. Similarly, less energy is charged and discharged in the case considering the off-design characteristics in winter, but the difference is smaller than that in the summer case. The minimum partial-load ratios of the compressor and turbine of the CAES considering the off-design characteristics are 61.2% and 49.0%, while those of the case without consideration are 56.6% and 36.4%, respectively. It can be seen that more compressors and turbines operate at the nominal load. Thus, in the winter, the difference between the cases with and without considering the off-design characteristics is smaller than in the summer. This is mainly due to the fact that more excess wind energy can be stored in the winter. Thus, it can be concluded that the off-design characteristics have much more of a side effect for the storage system when there is not enough renewable energy to be stored.

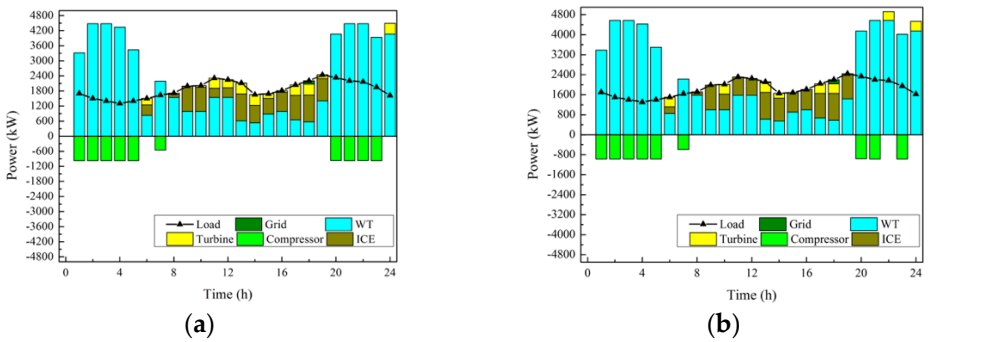

Figure 13. Operational power of electricity in winter: (**a**) without considering off-design characteristics; (**b**) considering off-design characteristics.

Figure 14 presents the operational power of the gas boiler and the exhaust heat of ICE. It can be seen that in Figure 14b the power of the ICE heat is higher than that of Figure 14a. As the operation power of the turbines is lower in the case considering the off-design characteristics, the operational power of ICE is higher than that of the case that does not consider the off-design characteristics.

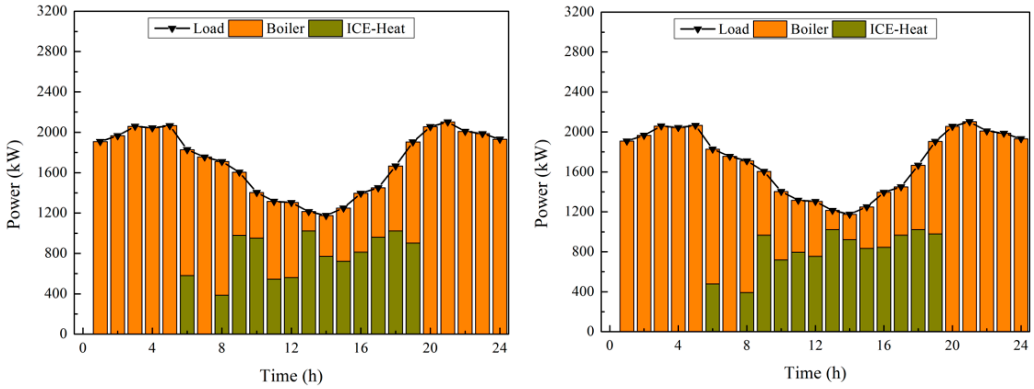

Figure 14. Operational power of heat in winter: (**a**) without considering off-design characteristics; (**b**) considering off-design characteristics.

For a further investigation, the partial-load ratio of ICE in each hour is presented in Figure 15. It can be seen that in the cases considering the off-design characteristics, the partial-load ratios of ICE are higher than those of the cases that do not consider the off-design at most of the times. As the result of there being more heat load in winter than cooling load in summer supplied by the ICE, the difference is more obvious in the winter conditions. Additionally, one can also draw the conclusion that the optimization method considering the off-design characteristics brings the devices (both CAES and ICE) closer to operation at the nominal load.

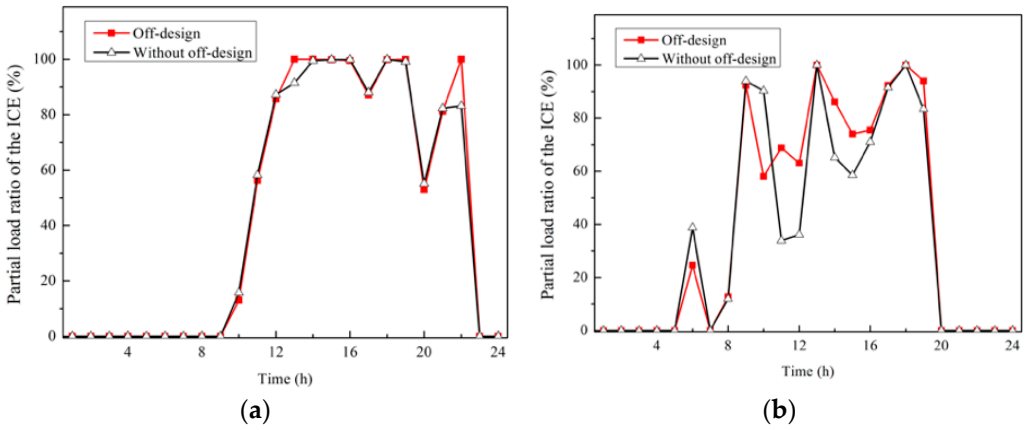

Figure 15. PLR of the ICE: (**a**) summer conditions; (**b**) winter conditions.

As the possibilities to carry out the experiments on a real full-scale system are limited, the model validation of CAES was carried out in comparison to the model in Ref. [34]. The results show that the model of the A-CAES system in this paper is correct and acceptable for off-design analysis and parameter-sensitive analysis. The effect of ambient temperature on the system performance is implemented with the same condition. Table 6 shows the model validation of the CAES system. It can be seen that the error between the two models is very small; so, the model of this paper can be regarded as acceptable.

Table 6. The comparison of the A-CAES model results from the present model and Ref. [34].

Parameters	Ref. [34]	The Present Model	Difference (%)
Power of compression train	25.2 MW	25.5 MW	1.2%
Power of expansion train	25.2 MW	25.3 MW	0.4%
Discharge time	16.75 h	16.75 h	0.0%
Charge time	12 h	12.02 h	0.2%
Efficiency	71.64%	71.16%	0.7%

5. Conclusions

In most studies on the optimization of HESs, the effects of the off-design operation of the components are neglected. This is problematic for the accuracy of the results, particularly when an energy storage system is part of a system to stabilize the energy output of a variety of renewable sources. This work investigated the impacts of the off-design operation of an A-CAES unit that was connected to a number of other energy-producing units in an HES, e.g., wind turbines and an ICE. A novel HES was proposed, and a bi-level optimization strategy was carried out for the study. The main objective was to optimize the economy of the HES by optimizing the capacity and operation strategy of each component. Then, a partial-load operation analysis showed how the performance of the system could be affected by deviating from the nominal-load conditions. The effects of different partial-load ratios of the system in winter and summer conditions were investigated. Then, the overall economy of the HES and the efficiency of the A-CAES were quantified. The study concludes with the following:

(1) The economy of the HES is highly affected by the off-design characteristics of A-CAES. The daily efficiency of the CAES unit is found to be 35% when considering its off-design characteristics, while it is as high as 51% otherwise. The off-design characteristics have a side effect on the system when obtaining an economic operation.
(2) When employing the bi-level optimization strategy, the strategy can reduce the impact of the off-design characteristics by increasing the capacity of the devices. The deviation of the operation costs between the cases with and without considering the off-design characteristics can decrease from 4.8% to 1.3%.
(3) The off-design characteristics of the compressor lead to the isentropic efficiency of the compressor falling dramatically, increasing the outlet air temperature. As a result of this, the off-design operation of the system also affects the temperature of the thermal storage chamber. The mean temperatures in the thermal storage chamber when considering and not-considering the off-design effects are at least 490 K and 475 K in winter and 457 K and 433 K in summer, respectively.
(4) For the optimization of the operation strategy, the SOC of the CAES is affected a lot by its off-design operation. The maximum SOCs of the chamber when considering the off-design characteristics are 10.9% in summer and 9.2% in winter, which are lower than those of the case when not considering the off-design characteristics, respectively. The efficiency differences of the A-CAES unit between the cases with and without considering the off-design features are 21% in summer and 8.9% in winter. The off-design characteristics also have impacts on the capacity of the components of the HES. When considering the off-design features, the rated power of the WTs becomes higher, while the rated power of the turbines becomes lower.

Author Contributions: Data curation, S.C.; Formal analysis, S.C.; Methodology, S.C.; Writing—original draft, S.C.; Writing—review & editing, A.A., G.C. and M.P.N. All authors have read and agreed to the published version of the manuscript.

Funding: Shanghai Science and technology innovation action plan (22YF1414900).

Institutional Review Board Statement: Not applicable.

Informed Consent Statement: Not applicable.

Data Availability Statement: Not applicable.

Acknowledgments: The work was supported by the Shanghai Science and technology innovation action plan (22YF1414900) "Research on intelligent control and multi energy conversion equipment of self-consistent integrated energy system".

Conflicts of Interest: The authors declare no conflict of interest.

Nomenclature

Symbols

V	volume, m^3
R_g	gas constant, J/(mol·K)
T	temperature, K
Q	thermal power, kW
P	electricity power, kW
L	load, kW
M	mass of air contained in the volume, kg
W	work, J
C	cost, USD
P	pressure, Pa
M	mass flow rate, kg/s
W	specific work, kJ/kg
C	specific heats, kJ/(kg·K)
T	time, h

Subscripts

C	Compressor
Ch	Chamber
T	Turbine
B	Boiler
A	Air
W	Water
V	Velocity
R	Ratio
Td	Total daily
Pl	Partial load
Ca	Capital
En	Environment
M	Motor
F	Rated power
Ele	Electricity cos
G	Generator
Op	Operation
Te	Thermal efficiency
Pe	Electrical efficiency
Jw	Jacket water
Ic	Intercool
$Loss$	Heat loss
Exh	Exhaust gas heat
Tur	Turbine
Com	Compressor
E	Electricity
He	Heat exchanger
Re	Recovery
Ac	Absorbed chiller
Ec	Electricity chiller

Greek letters	
Π	Pressure ratio
H	Efficiency
E	Heat exchanger effectiveness
A	Partial-load ratio
Acronyms	
CAES	compressed air energy storage
A-CAES	adiabatic-CAES
TES	thermal energy storage
SOC	state of charge
ICE	internal combustion engine
WT	wind turbine
DE	differential evaluation
O&M	operation and maintenance

References

1. Wang, K.X.; Chen, S.; Liu, L.C.; Zhu, T.; Gan, Z.X. Enhancement of renewable energy penetration through energy storage technologies in a CHP-based energy system for Chongming, China. *Energy* **2018**, *162*, 988–1002. [CrossRef]
2. Luo, X.; Wang, J.H.; Krupke, C.; Wang, Y.; Sheng, Y.; Li, J.; Xu, Y.J.; Wang, D.; Miao, S.H.; Chen, H.S. Modelling study, efficiency analysis and optimisation of large-scale Adiabatic Compressed Air Energy Storage systems with low-temperature thermal storage. *Appl. Energy* **2016**, *162*, 589–600. [CrossRef]
3. Hartmann, N.; Vohringer, O.; Kruck, C.; Eltrop, L. Simulation and analysis of different adiabatic Compressed Air Energy Storage plant configurations. *Appl. Energy* **2012**, *93*, 541–548. [CrossRef]
4. Chen, S.; Arabkoohsar, A.; Zhu, T.; Nielsen, M.P. Development of a micro-compressed air energy storage system model based on experiments. *Energy* **2020**, *197*, 117–130. [CrossRef]
5. Khaitan, S.K.; Raju, M. Dynamics of hydrogen powered CAES based gas turbine plant using sodium alanate storage system. *Int. J. Hydrog. Energy* **2012**, *37*, 18904–18914. [CrossRef]
6. Chen, L.J.; Zheng, T.W.; Mei, S.W.; Xue, X.D.; Liu, B.H.; Lu, Q. Review and prospect of compressed air energy storage system. *J. Mod. Power Syst. Clean Energy* **2016**, *4*, 529–541. [CrossRef]
7. Zhao, P.; Wang, M.K.; Wang, J.F.; Dai, Y.P. A preliminary dynamic behaviors analysis of a hybrid energy storage system based on adiabatic compressed air energy storage and flywheel energy storage system for wind power application. *Energy* **2015**, *84*, 825–839. [CrossRef]
8. Ibrahim, H.; Younes, R.; Ilinca, A.; Dimitrova, M.; Perron, J. Study and design of a hybrid wind-diesel-compressed air energy storage system for remote areas. *Appl. Energy* **2010**, *87*, 1749–1762. [CrossRef]
9. Arabkoohsar, A.; Machado, L.; Farzaneh-Gord, M.; Koury, R.N.N. The first and second law analysis of a grid connected photovoltaic plant equipped with a compressed air energy storage unit. *Energy* **2015**, *87*, 520–539. [CrossRef]
10. Arabkoohsar, A.; Ismail, K.A.R.; Machado, L.; Koury, R.N.N. Energy consumption minimization in an innovative hybrid power production station by employing PV and evacuated tube collector solar thermal systems. *Renew. Energy* **2016**, *93*, 424–441. [CrossRef]
11. Li, Y.; Miao, S.; Luo, X.; Yin, B.; Han, J.; Wang, J. Dynamic modelling and techno-economic analysis of adiabatic compressed air energy storage for emergency back-up power in supporting microgrid. *Appl. Energy* **2020**, *261*, 114448. [CrossRef]
12. Razmi, A.R.; Janbaz, M. Exergoeconomic assessment with reliability consideration of a green cogeneration system based on compressed air energy storage (CAES). *Energy Convers. Manag.* **2020**, *204*, 112320. [CrossRef]
13. Sadreddini, A.; Fani, M.; Aghdam, M.A.; Mohammadi, A. Exergy analysis and optimization of a CCHP system composed of compressed air energy storage system and ORC cycle. *Energy Convers. Manag.* **2018**, *157*, 111–122. [CrossRef]
14. Mohammadi, A.; Ahmadi, M.H.; Bidi, M.; Joda, F.; Valero, A.; Uson, S. Exergy analysis of a Combined Cooling, Heating and Power system integrated with wind turbine and compressed air energy storage system. *Energy Convers. Manag.* **2017**, *131*, 69–78. [CrossRef]
15. Zhang, X.J.; Chen, H.S.; Xu, Y.J.; Li, W.; He, F.J.; Guo, H.; Huang, Y. Distributed generation with energy storage systems: A case study. *Appl. Energy* **2017**, *204*, 1251–1263. [CrossRef]
16. Yan, Y.; Zhang, C.H.; Li, K.; Wang, Z. An integrated design for hybrid combined cooling, heating and power system with compressed air energy storage. *Appl. Energy* **2018**, *210*, 1151–1166. [CrossRef]
17. Yao, E.R.; Wang, H.R.; Wang, L.G.; Xi, G.; Marechal, F. Thermo-economic optimization of a combined cooling, heating and power system based on small-scale compressed air energy storage. *Energy Convers. Manag.* **2016**, *118*, 377–386. [CrossRef]
18. Yao, E.R.; Wang, H.R.; Wang, L.G.; Xi, G.; Marechal, F. Multi-objective optimization and exergoeconomic analysis of a combined cooling, heating and power based compressed air energy storage system. *Energy Convers. Manag.* **2017**, *138*, 199–209. [CrossRef]
19. Rouindej, K.; Samadani, E.; Fraser, R.A. A comprehensive data-driven study of electrical power grid and its implications for the design, performance, and operational requirements of adiabatic compressed air energy storage systems. *Appl. Energy* **2020**, *257*, 113990. [CrossRef]

20. Guo, H.; Xu, Y.; Guo, C.; Zhang, Y.; Hou, H.; Chen, H. Off-design performance of CAES systems with low-temperature thermal storage under optimized operation strategy. *J. Energy Storage* **2019**, *24*, 100787. [CrossRef]
21. Chen, S.; Rahbari, H.R.; Arabkoohsar, A.; Zhu, T. Impacts of Partial-Load Service on Energy, Exergy, Environmental and Economic Performances of Low-Temperature Compressed Air Energy Storage System. *J. Energy Storage* **2020**, *32*, 101900. [CrossRef]
22. Mazloum, Y.; Sayah, H.; Nemer, M. Dynamic modeling and simulation of an Isobaric Adiabatic Compressed Air Energy Storage (IA-CAES) system. *J. Energy Storage* **2017**, *11*, 178–190. [CrossRef]
23. Meng, H.; Wang, M.; Olumayegun, O.; Luo, X.; Liu, X. Process design, operation and economic evaluation of compressed air energy storage (CAES) for wind power through modelling and simulation. *Renew. Energy* **2019**, *136*, 923–936. [CrossRef]
24. Arabkoohsar, A.; Alsagri, A.S.; Alrobaian, A.A. Impact of Off-design operation on the effectiveness of a low-temperature compressed air energy storage system. *Energy* **2020**, *197*, 117–176. [CrossRef]
25. Alsagri, A.S.; Arabkoohsar, A.; Rahbari, H.R.; Alrobaian, A.A. Partial load operation analysis of trigeneration subcooled compressed air energy storage system. *J. Clean. Prod.* **2019**, *238*, 117948. [CrossRef]
26. Li, Y.W.; Miao, S.H.; Yin, B.X.; Yang, W.C.; Zhang, S.X.; Luo, X.; Wang, J.H. A real-time dispatch model of CAES with considering the part-load characteristics and the power regulation uncertainty. *Int. J. Electr. Power Energy Syst.* **2019**, *105*, 179–190. [CrossRef]
27. Zhao, P.; Gao, L.; Wang, J.; Dai, Y. Energy efficiency analysis and off-design analysis of two different discharge modes for compressed air energy storage system using axial turbines. *Renew. Energy* **2016**, *85*, 1164–1177. [CrossRef]
28. Yang, K.; Zhang, Y.; Li, X.M.; Xu, J.Z. Theoretical evaluation on the impact of heat exchanger in Advanced Adiabatic Compressed Air Energy Storage system. *Energy Convers. Manag.* **2014**, *86*, 1031–1044. [CrossRef]
29. Jubeh, N.M.; Najjar, Y.S.H. Green solution for power generation by adoption of adiabatic CAES system. *Appl. Therm. Eng.* **2012**, *44*, 85–89. [CrossRef]
30. He, Y.; Chen, H.S.; Xu, Y.J.; Deng, J.Q. Compression performance optimization considering variable charge pressure in an adiabatic compressed air energy storage system. *Energy* **2018**, *165*, 349–359. [CrossRef]
31. Chen, S.; Arabkoohsar, A.; Yang, Y.; Zhu, T.; Nielsen, M.P. Multi-objective optimization of a combined cooling, heating, and power system with subcooled compressed air energy storage considering off-design characteristics. *Appl. Therm. Eng.* **2021**, *187*, 116562. [CrossRef]
32. Storn, R.; Price, K. Differential evolution—A simple and efficient heuristic for global optimization over continuous spaces. *J. Glob. Optim.* **1997**, *11*, 341–359. [CrossRef]
33. Chen, S.; Zhu, T.; Zhang, H.Y. Study on optimization of pressure ratio distribution in multistage compressed air energy storage system. *J. Energy Resour. Technol.-Trans.* **2019**, *141*, 10. [CrossRef]
34. Zhao, P.; Dai, Y.P.; Wang, J.F. Design and thermodynamic analysis of a hybrid energy storage system based on A-CAES (adiabatic compressed air energy storage) and FESS (flywheel energy storage system) for wind power application. *Energy* **2014**, *70*, 674–684. [CrossRef]